TWNK in Parkinson's disease: a Movement Disorder and Mitochondrial Disease Center perspective study

- Supplementary Materials -

Index

Abbreviations: AA = amino acids; ACMG = American College of Medical Genetic; AD = Autosomal Dominant; adPEO = autosomal dominant Progressive External Ophthalmoplegia; adPEO-P = adPEO with parkinsonism; AR = Autosomal Recessive; Ch. position = Chromosomal position; COX = Cytochrome C Oxidase; EOPD = Early Onset Parkinson's disease; F = female; Het = Heterozygous (monoallelic); LB = Likely Benign; LP = Likely Pathogenic; M = male; Mamm. cons. = Mammalian conservation; MIRAS = Mitochondrial Recessive Ataxia Syndrome; MLPA = Multiple Ligation Probe Amplification; MT = MutationTaster2021; mtDNA = mitochondrial DNA; NA = Not assessed; NGS = Next Generation Sequencing; Not K = not known; OSAS = Obstructive Sleep Apnea Syndrome; P = Pathogenic; PCR = Polymerase Chain Reaction; PD = Parkinson's disease; PEO = Progressive External Ophthalmoplegia; PP-2 = PolyPhen-2; RBD = REM-sleep behaviour disorder; rs# = rs number; SANDO = Sensory Ataxia Neuropathy Dysarthria and Ophthalmoplegia; VUS = Variant of Unknown Significance; VUS-LP = VUS with likely pathogenic effect; VUS-P = VUS with pathogenic effect; WES = Whole Exome Sequencing

Supplementary Methods

All patients with diagnosis of Parkinson's disease (PD) were evaluated at the Movement Disorders Center of the IRCCS Foundation Ca' Granda Ospedale Maggiore Policlinico (Milan, Italy) and Istituto di Ricovero e Cura a Carattere Scientifico Humanitas (Rozzano, Italy). Video-oculography was performed in two PD patients to assess the presence of subclinical gaze limitation.

A venous blood sample was collected with standard procedures. Genomic DNA was extracted from total peripheral blood with standard procedures in both cohorts.

All *TWNK* variants (ENST00000311916.8, NM_021830.5, Q96RR1) were validated by Sanger sequencing. Variants were classified according to ACMG criteria[1]. Online databases were consulted to assess previous association of variants with disease (ClinVar), mammalian conservation, allele frequency in European (Finnish, non-Finnish) population (gnomAD v2.1.1). Variants of unknown significance (VUS) were further classified according to their potential pathogenicity, and VUS classified as "pathogenic" or "likely pathogenic" (VUS-P or VUS-LP) were retained[2]. *TWNK* variants classified as Benign or Likely Benign according to ACMG criteria were not considered for further analysis.

mtDNA deletions and copy number

In the PD cohort, mtDNA copy number was quantitatively assessed in four *TWNK*-PD patients from venous blood samples through RealTime-PCR and was compared to 176 age and sex-matched controls. In the adPEO cohort, mtDNA deletions, DNA 7S[3] and copy number[4] were assessed on available skeletal muscle biopsies derived from patients with or without parkinsonism (controls $n = 5$, *TWNK*-adPEO $n = 10$, *TWNK*-adPEO-P $n = 2$).

Statistical analysis

Differences between *TWNK*-PD and *TWNK*-adPEO-P patients were evaluated with the chi-square test. Differences among *TWNK*-adPEO patients with or without parkinsonism and controls were evaluated by 1-way ANOVA with Tukey's multiple comparisons test. A p-value (P) of 0.05 was set to obtain statistical significance.

Protein structure modeling

The monomeric structure of human TWINKLE was generated in AlphaFold and molecular modeling was performed in ChimeraX[5,6]. The monomer was aligned with the structure of the closely related gp4 protein from T7 bacteriophage (PDB ID: 1Q57). The hexamer lacking the N-terminal domain was built with the help of the hexameric structure of the gp4 protein using six monomers of TWINKLE. The C-terminus sequence alignment (residues 629-684, unstructured in the structure) was made in Clustal Omega (https://www.ebi.ac.uk/Tools/msa/clustalo/).

Clinical reports

TWNK-PD patients

Patient 1 is a 58-year-old Italian male diagnosed with idiopathic PD at the age of 50. Onset of motor symptoms was with painful rigidity of the right shoulder and slowness of the right hand. He had a good response to dopamine agonist treatment, but experienced impulse control disorder (excessive computer use) and was shifted to levodopa with benefit. He developed motor fluctuations at the age of 54 and dyskinesia at 57 years. Hyposmia and rem-behavior disorder (RBD) were reported at the age of the diagnosis. In his past medical history, he reported epilepsy since the age of 20, initially treated with valproate, which he discontinued apparently without specific reason. After a long remission of 26 years, he had convulsive epileptic status treated with levetiracetam. Brain MRI showed small nonspecific white matter lesions. He also reported an episode of Bell's palsy at the age of 30. Family history was negative for neurological diseases, he has no siblings and his parents died at young age for neoplastic and hepatic diseases. His neurological examination shows extrapyramidal signs with moderate dyskinesia, without evidence of ptosis, eye movement impairment or muscular weakness. Video-oculography confirmed normal eye tracking movements. Blood analysis showed a slight but consistent increment of serum creatine phosphokinase levels (250 U/l, normal range 37-189 U/l).

Patient 2 is a 44-year-old Italian male diagnosed with early-onset PD (EOPD) at the age of 42. He reported slowness of movement of the right limbs and mild rest tremor on the right hand. Neurological assessment showed mild bradykinesia of the right limbs and rest tremor on the right hand with bilateral cogwheel rigidity; muscle involvement, eyelid ptosis or abnormalities of ocular movements were not present. He is currently treated with dopamine agonist therapy with good response. Non-motor symptoms were hyposmia and RBD. In his

medical history there is familial adenomatous polyposis, treated with colectomy with ileorectal anastomosis. Neurological family history is remarkable for motor slowness in his maternal aunt, without a formal diagnosis of PD.

Patient 3 is a 63-year-old woman who reported motor slowness of her left upper limb at the age of 38. Her family history was negative for neurological disorders. She has a 58-year-old brother with no neurological complaints. She had excellent and sustained response to levodopa. She developed motor fluctuations and intense dyskinesias. Bilateral palpebral ptosis and oculomotor limitations were not observed during neurological assessment. Brain MRI was unremarkable.

Patient 4 is a 65-year-old woman who came to our attention for the onset of right-hand tremor since the age of 61. Neurological examination revealed mild hypomimia, mild bradykinesia and rest tremor in her right hand. Ocular movements were unremarkable. She had an excellent response to levodopa and dopamine agonist treatment. She reported constipation and orthostatic hypotension, exacerbated by the introduction of levodopa therapy. She underwent 123I FP-CIT SPECT (DaTScan) with evidence of marked bilateral reduction of putaminal uptake with prevalence on the left side. Idiopathic PD was diagnosed. In her past medical history, she reported the occurence of bilateral eyelid ptosis since the middle young age, for which she underwent corrective eyelid surgery at age 54. Serum creatine phosphokinase level was normal as well as the electromyography. She underwent an eye tracking analysis that confirmed normal eye movement velocity. Her mother was affected by eyelid ptosis that was surgically treated and developed akinetic-rigid PD at the age of 60.

Patient 5 is an Italian female who suffered from bradykinesia and rigidity on the left side since the age of 65. She was diagnosed with idiopathic PD. She reported constipation and hyposmia a few years prior to the motor symptoms onset. Brain MRI showed small

nonspecific white matter lesions. She obtained clinical benefits from dopamine-agonist therapy. She was also affected from bilateral palpebral ptosis since younger age. She was treated with acetylcholinesterase inhibitors with no benefit. Antibodies anti-AchR and anti-MuSK were negative. Serum creatine phosphokinase level was normal as well as the electromyography. No ophthalmoplegia was detected at the neurological examination.

Patient 6 is a 75-year-old woman who came to our attention for the presence of resting tremor at her right upper limb at the age of 60. She also suffered from rigidity and dystonia. Sustained levodopa response was obtained. During the years she developed motor fluctuations and dyskinesias. Her past medical history was remarkable for cardiac arrhythmia and hypertension. Her parents are first cousins and one of her sisters suffers from postural tremor of the upper limbs. No bilateral palpebral ptosis and limitations of gaze were observed during the neurological examination.

TWNK-adPEO-P patients

Patient 7 is a 74-year-old male who developed progressive bilateral ptosis at the age of 60. He started to suffer from progressive bilateral bradykinesia at least ten years after the ocular involvement. His past medical history was noticeable for depression. Asymmetrical bilateral ptosis (left > right), bilateral ophthalmoplegia, proximal muscle weakness of the lower limbs, hypomimia, monotone speech, plastic hypertonia at four limbs, bradykinesia (left > right), postural tremor at upper limbs, reduced pendular movements of upper limbs (left > right), and camptocormia were observed at neurological examination. Brain CT was normal, whereas brain MRI showed cortical atrophy and basal ganglia T1 hypointensity. Cerebral MR spectroscopy demonstrated a lactate peak. Muscular involvement was assessed with electromyography (which disclosed a myopathic pattern) and muscle biopsy (which showed myopathic features with COX negative fibers). Lactic acid after standardized effort resulted

abnormal (35.7 mg/dL). An attempt with L-DOPA treatment was not well tolerated and the patient was lost at follow-up.

Patient 8 is a 88-year-old female who developed bilateral ptosis with double vision at the age of 49. At the age of 60 she also developed progressive proximal muscle weakness. At 69 she presented difficulties in swallowing solids and liquids. When she was 75-year-old she developed camptocormia and head tremor for which she was never treated. Her past medical history was remarkable for type II diabetes, glaucomatous optic atrophy, and hypertension. Bilateral ptosis with ophthalmoplegia, myopathic face and proximal weakness of upper and lower limbs, hypomimia, head tremor, reduced pendular movements of upper limbs, and camptocormia were observed during the neurological assessment. Brain CT revealed basal ganglia calcifications, whereas brain MRI showed chronic vascular encephalopathy. Muscular involvement was assessed with electromyography (EMG), which documented a myopathic pattern in the examined muscles. Lactic acid after standardized effort resulted abnormal (26 mg/dL).

Patient 9 is a 86-year-old female who reported a slowly progressive bilateral ptosis since she was young. At 82 she developed a progressive bradykinesia. Her past medical history revealed hypercholesterolemia and hypertension. Neurological examination showed bilateral ptosis with ophthalmoplegia, apraxia, mild plastic hypertonia, bradykinesia prevalent on left side, and reduced pendular movements on the left side. DaTScan demonstrated a mild bilateral alteration of the nigro-striatal system. Brain CT was normal. The patient refused the option of therapy with L-DOPA.

Patient 10 is a 77-year-old female who developed a slowly progressive bilateral ptosis at 39. At 69 she also developed a progressive bradykinesia. Her past medical history disclosed hypertension, glucose intolerance, hypothyroidism, depression, and OSAS. Bilateral ptosis

with ophthalmoplegia, mild plastic hypertonia at the four limbs (right > left), bradykinesia, and camptocormia were observed at neurological examination. DaTScan was assessed twice (at 69 and 76y), both times resulting negative for nigrostriatal degeneration. Brain MRI showed cortical atrophy and chronic vascular encephalopathy. Cerebral MR spectroscopy showed no presence of lactate. Muscular involvement was assessed with EMG (normal) and muscle biopsy (rare COX negative fibers).

Patient 11 is a 80-year-old female with bilateral ptosis (onset undefined) and sensorineural deafness. At 72 she reported the onset of hypophonia, micrography and rigidity at upper limbs. In her past medical history, there was hypertension and hypothyroidism. Neurological examination showed bilateral ptosis with ophthalmoplegia, proximal weakness of the lower limbs, hypomimia, hypophonia, plastic hypertonia of the upper limbs (right > left) and axial, bradykinesia, and camptocormia. DatScan showed moderate bilateral alterations of the nigro-striatal system. Brain CT was normal, whereas brain MRI showed cortical atrophy and chronic vascular encephalopathy. Muscular involvement was assessed with EMG, which resulted normal. A therapy with L-DOPA was started at age 76, which was discontinued due to poor response.

Structural analysis

In-silico analysis was performed to assess if variants associated with PD could impact the structure and function of TWINKLE. The structure of TWINKLE has not been experimentally solved, but several structures of the homologous gp4 primase–helicase from bacteriophage T7 are available. The overall sequence similarity between TWINKLE and gp4 is about 46% (with 15% sequence identity)[7]. To assess the functional consequences of PD variants, we used AlphaFold in combination with homology modeling on the structure of gp4 (Fig. S3 A and B)[5,6]. In spite of limited sequence similarities between N-terminal part of TWINKLE and gp4, the predicted structures of the two are closely related. L167 is located in a loop pointing inwards, forming a network of multiple hydrophobic interactions with nearby aliphatic amino acids (indicated in red). Substituting the hydrophobic Leu with a branched and flexible side chain with the rigid amino acid Pro will disturb these hydrophobic interactions, which may decrease protein stability and loss of activity (Fig. S3 C). In addition, together with the adjacent amino acids at positions 168 and 169, the mutation forms a Pro-Pro-Asp motif, which often results in ribosome stalling in mammalian cells[8]. R371 is located in an α-helix in the TWINKLE linker region (Fig. S3 D, pink residue). This α-helix is important for connecting one TWINKLE monomer to the neighboring monomer (purple α-helix) and several known PEO mutations S369P, R374Q, and L381P (Fig S3 D, green residues) are located in the same α-helix[7]. A change from Arg to a Gln at position 371 will abolish the possibility to form a salt bridge with E479 and likely provoke a destabilization of the hexamer. E461K and G540R are located in the helicase domain, close to previously characterized disease-causing mutations (E461 is close to A460G, A460P, R463W (Fig S3 E, green residues), and G540 to Y537H, situated within the same α-helix (Fig S3 F, pink respective green residues)[9]. Glu at position 461 makes a salt bridge with R394 (Fig S3 E), dashed line represents 1.9 Å). Introducing a Lys will break this interaction but also introduce a positive charge that will repulse the positively charged arginine leading to structural deformation (Fig S3 E, right panel). A similar rationale as for E461K can be used for amino acid substitution G540R (Fig S3 F, pink residue). Please note that Gly is the simplest amino acid with no sidechain and therefore only indicated as a pink surface in the α-helix. The extended side chain of the positively charged Arg clashes with Lys at position 578 (Fig S3 F, red residue), resulting in a possible destabilization of the protein. The last two PD variants, p.K656Q and p.Q670H, are located in the unstructured C-terminal part of the protein, making it more difficult to predict the effect of the mutations. However, the residues are conserved in

mammals (Fig S3 G, labeled pink), supporting essential functions. Interestingly the C-terminal (the last 21 residues) in gp4 is also unstructured and is critical for interactions with the T7 DNA polymerase during leading-strand synthesis[10,11]. The C-terminal part of TWINKLE most likely plays a similar function. In support of this, several conserved residues close to K656Q and Q670H (Fig S3 G, labeled green) are known to cause mitochondrial disease (https://www.ncbi.nlm.nih.gov/clinvar/). In conclusion, the molecule modeling supports that all six mutations identified in PD patients affect TWINKLE structure and as a consequence, most likely activity, explaining the pathogenic phenotype.

Supplementary Tables

Supplementary Table 1 (Table S1)

List of genes included in the targeted or virtual NGS panel.

Gene	Transcript ID	UniProt ID	RefSeq	Inheritance
SNCA	ENST00000394991.8	P37840	NM_000345.4	AD
LRRK2	ENST00000298910.12	Q5S007	NM_198578.4	AD
VPS35	ENST00000299138.12	Q96QK1	NM_018206.6	AD
GBA	ENST00000368373.8	P04062	NM_000157.4	AD, risk factor
RAB39B	ENST00000369454.4	Q96DA2	NM_171998.4	X-linked
PRKN	ENST00000366898.6	O60260	NM_004562.3	AR
PINK1	ENST00000321556.5	Q9BXM7	NM_032409.3	AR
DJ-1	ENST00000338639.10	Q99497	NM_007262.5	AR
ATP13A2	ENST00000326735.13	Q9NQ11	NM_022089.4	AR
PLA2G6	ENST00000332509.8	O60733	NM_003560.4	AR
DNAJC6	ENST00000371069.5	O75061	NM_001256864.2	AR
SYNJ1	ENST00000433931.7	J3KQV8	NM_003895.3	AR
FBXO7	ENST00000266087.12	Q9Y3I1	NM_012179.4	AR
VPS13C	ENST00000644861.2	Q709C8	NM_020821.3	AR
PTRHD1	ENST00000328379.6	Q6GMV3	NM_001013663.2	AR
POLG	ENST00000268124.11	E5KNU5 P54098	NM_002693.3	AD, AR
TWNK	ENST00000311916.8	Q96RR1-1	NM_021830.5	AD, AR
OPA1	ENST00000361510.8	O60313-10	NM_130837.3	AD, AR
SLC25A46	ENST00000355943.8	Q96AG3-1	NM_138773.4	AR

Supplementary Table 2 (Table S2)

Genetic data of all *TWNK* variants identified in the adPEO cohort (18 of 302 patients).

Genetic data, minor allele frequency in Europeans (based on gnomAD v2.1.1), clinical significance (based on ClinVar), ACMG criteria and classification are shown for each *TWNK* variant identified from the adPEO cohort.

# Pts	Ch. Position (chr10:)	Base change	AA change	Zygosity	Protein impact	Mamm. Cons.	dbSNP (rs#)	gnomAD[a]	ClinVar	ACMG Criteria[b]	Classification[c]
n=5	102748874C>T	c.907C>T	p.R303W	Het	Missense	Yes	rs1159929268	1/113,466 (0.000008813)	-	PM1m PM5m PP5m, PM2su PP2su, PP3su	LP
n=1	102748875G>A	c.908G>A	p.R303Q	Het	Missense	Yes	rs137852956	2/113,500 (0.0000176)	VUS	PM1m PM5m PM2su, PP2su, PP3su, PP5su	LP
n=4	102748968G>A	c.1001G>A	p.R334Q	Het	Missense	Yes	rs28937887	-	P	PM1m, PP5s PM5m, PM2su, PP2su, PP3su BP6su	P
n=1	102748968G>T	c.1001G>T	p.R334L	Het	Missense	Yes	rs28937887	-	-	PM1m, PM5s PM2su, PP2su, PP3su	LP
n=1	102749042G>A	c.1075G>A	p.A359T	Het	Missense	Yes	rs111033573	-	P	PM1s, PS3s PM2su, PP2su, PP3su	P
n=1	102749076T>A	c.1109T>A	p.F370Y	Het	Missense	Yes	-	-	-	PM1s, PM2s PM5s, PP2su PP3su	P
n=1	102749139G>A	c.1172G>A	p.R391H	Het	Missense	No	rs556445621	3/113,676 (0.00002639)	LB	PM1m, PP5s PM2su, PP2su, PP3su BP6su	LP

										ACMG criteria	Classification
n=2	102749434G>A	c.1277G>A	p.S426N	Het	Missense	Yes	-	-	-	PM1m, PM2s PP2su, PP3su PP5su	LP
n=1	102750642T>C	c.1609T>C	p.Y537H	Het	Missense	Yes	rs144001072	33/113,770 (0.0002941)	VUS	PM1m, PM2su PP2su, BP4su	VUS-LP
n=1	102753093delTTC	c.1882_1884 delTTC	p.F628del	Het	Deletion	Yes	rs761514855	1/113,768 (0.00000879)	-	PM1m, PM2s PM4m, PP3su	LP

[a]Allele frequency in European (non-Finnish) population. All variants were absent in European (Finnish) population. [b]ACMG criteria: vs = very strong; s = strong; m = moderate; su = supporting. [c]Classification: VUS = Variant of Unknown Significance; VUS-LP = VUS with likely pathogenic effect; VUS-P = VUS with pathogenic effect; LP = Likely Pathogenic; P = Pathogenic.

Supplementary Table 3 (Table S3)

Demographic, clinical, and genetic features of *TWNK*-PD and *TWNK*-adPEO-P patients.

	TWNK-PD						*TWNK*-adPEO-P				
Case number (#)	Patient 1	Patient 2	Patient 3	Patient 4	Patient 5	Patient 6	Patient 7	Patient 8	Patient 9	Patient 10	Patient 11
Gender	M	M	F	F	F	F	M	F	F	F	F
Family history (PEO and/or PD)	No	Yes (motor slowness)	No	Yes (PD)	No	Yes (postural tremor)	Not K	Not K	Not K	Not K	Not K
Age at onset (y) of PEO	-	-	-	Young age (palpebral ptosis)	Young age (palpebral ptosis)	-	60 (palpebral ptosis)	49	Juvenile age (palpebral ptosis)	39 (palpebral ptosis)	Not datable

Age at onset (y) of extrapyramidal symptoms	50	42	38	61	65	60	71	75	82	69	72
Palpebral ptosis	-	-	-	+	+	-	+	+	+	+	+
External ophthalmoplegia	-	-	-	-	-	-	+	+	+	+	+
Muscle weakness	-	-	-	-	-	-	+	+	-	-	+
Bradykinesia and rigidity	+	+	+	+	+	+	+	-	+	+	+
Resting tremor	-	+	-	+	-	+	-	-	-	-	-
Dopa response	+	+	+	+	+	+	-	NA	NA	NA	-
Motor fluctuations	+	NA	+	NA	NA	+	-	-	-	-	-
Dyskinesias	+	NA	+	NA	NA	+	-	-	-	-	-
Falls	-	-	-	-	-	-	-	-	-	-	-
Psychiatric symptoms	-	-	-	-	-	-	Depression	-	-	Depression	-
Other features	Epilepsy, iperCPK	-	-	-	-	Dystonia	Postural tremor, abnormal lactic acid after standardized effort	Dysphagia, head tremor, type II diabetes, glaucomatous optic atrophy, abnormal lactic acid after standardized effort	Apraxia	Glucose intolerance, OSAS	Sensorineural deafness
Brain MRI	Small, non-specific white matter lesions	NA	Normal	NA	NA	NA	Cortical atrophy, basal ganglia T1 hypointensity; lactate at spectroscopy	Chronic vascular encephalopathy, basal ganglia calcifications at brain CT	Normal (CT)	Cortical atrophy, chronic vascular encephalopathy	Cortical atrophy, chronic vascular encephalopathy

DaTScan	NA	NA	NA	+	NA	NA	NA	NA	+	-	+
Muscle biopsy And EMG pattern	NA	NA	NA	NA	NA	NA	Myopathic with COX negative fibers; myopathic pattern at EMG	NA, myopathic pattern at EMG	NA, normal pattern at EMG	Rare COX negative fibers; normal pattern at EMG	NA, normal pattern at EMG
TWNK variants	c.500T>C, p.L167P, het	c.1112G>A, p.R371Q, het	c.1381G>A, p.E461K, het	c.1618G>A, p.G540R, het	c.1966A>C, p.K656Q, het	c.2010G>C, p.Q670H, het	c.907C>T, p.R303W,het		c.1001G>A, p.R334Q, het		c.1609T>C, p.Y537H, het
Classification (ACMG criteria[1,2])	LP	LP	LP	P	VUS-LP	VUS-LP	LP		P		VUS-LP
Additional variants	-	-	-	*PRKN* p.R275W het, *ATP13A2* p.V1137M het	-	-	-	-	-	-	-

4.4 Supplementary Table 4 (Table S4)

Demographic, clinical, and genetic features of previously reported cases of parkinsonism associated to *TWNK* variants.

Reference	Van Goethem et al.[12]	Baloh et al.[13]			Liu et al.[14]	Vandenberghe et al.[15]	Brandon et al.[16]	Kiferle et al.[17]		Breen et al.[18]
Case number (#)	1	2	3	4	5	6	7	8	9	10
Gender	F	F	F	F	F	M	M	F	F	M
Nationality	NA	NA	NA	NA	Chinese	Flemish	NA	Italian	Italian	NA
Family history (PEO and/or PD)	No	Yes (both)	Yes (both)	Yes (both)	Yes (PEO)	Yes (PEO)	No	Yes (both)	Yes (both)	Yes (PD)

Age at onset (y) of PEO	52	30	20	30	30	30	64	Childhood	45	< 58
Age at onset (y) of extrapyramidal symptoms	52	50	41	40	57	50	70	< 80	77	59
Palpebral ptosis	+	+	+	+	+	+	+	+	+	+
External ophthalmoplegia	+	+	+	+	+	+	+	+	+	+
Muscle weakness	+	+	-	-	-	-	-	-	-	-
Bradykinesia and rigidity	+	+	+	+	+	+	+	+	+	+
Resting tremor	+	+	+	+	-	+	+	+	+	+
Dopa response	+	NA	+	+	-	NA	NA	+	NA	+
Motor fluctuations	NA	NA	NA	NA	-	NA	NA	NA	NA	+
Dyskinesias	NA	NA	NA	NA	-	NA	NA	NA	NA	+
Falls	-	+	-	-	-	-	-	+	-	+
Psychiatric symptoms	Depression	-	Bipolar disorder	-	-	-	-	Depression	-	Visual hallucinations and paranoia
Other features	Dysphagia, dysarthria, generalized myopathy	Axonal sensory-motor polyneuropathy	-	-	-	-	-	Sensorineural hypoacusis, nocturnal apneas, postural tremor, cognitive impairment	Mandibular tremor, postural tremor, reduced tendon reflexes	Cognitive decline, dysphagia
Brain MRI	Normal (CT)	NA	Normal	NA	Lacunar infarction in basal ganglia	Normal	Mild, non-specific white matter lesions	Mild white matter encephalopathy and atrophy	NA	Mild, non-specific white matter lesions
DaTScan	NA	NA	NA	NA	NA	+	+	+	+	NA

Muscle biopsy	Mitochondrial proliferation, ragged red fiber, mtDNA deletions	NA	Mitochondrial proliferation, COX-negative fibers, mtDNA deletions	NA	NA	Normal	Predominance of type II fibers, numerous central nuclei, COX-negative fibers, mtDNA deletions	NA	Ragged red and blue fibers, COX-negative fibers	NA
TWNK variants	c.1031G>A, p.R334Q, het	c.1121G>A, p.R374Q, het			c.1423G>A, p.A475T, het	c.1031G>A, p.R334Q, het	c.907C>T, p.R303W, het	c.1750G>A, p.A359T, het		c.908G>A, p.R303Q, het
Additional variants	*POLG* p.G848S het	-	-	-	-	-		-	-	-

Supplementary Figures

Supplementary Figure 1 (Fig. S1)

Box plot showing blood cells mtDNA content in *TWNK*-PD patients (*n*=4) compared with healthy controls (*n*=176). Solid bars represent median values. mtDNA quantification, normalized to nuclear DNA (nDNA) content, was performed by quantitative real-time PCR as previously described[19]. Mitochondrial DNA content in TWNK-PD was not significantly altered compared to control subjects (t-test, $P = 0.13$).
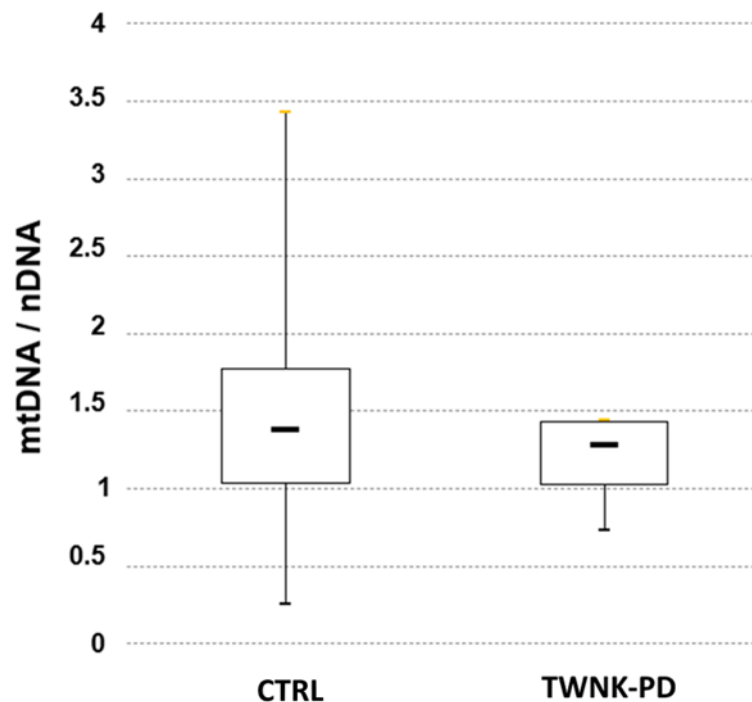
Supplementary Figure 2 (Fig. S2)

Scatter plot showing skeletal muscle mtDNA content per cell, deletion quantification (ND4/ND1 ratio) and 7S DNA quantification (DNA 7S/mtDNA ratio) in *TWNK*-adPEO (*n*=10) and *TWNK*-adPEO-P patients (*n*=2) compared with healthy controls (CTRL, *n*=5). Data were presented as scatter plot with median values and standard deviation. The

mtDNA assets were evaluated by mtDNA quantification (upper panel), mtDNA deletions (central panel), expressed as ratio between MT-ND4 (major arc) and MT-ND1 (minor arc) genes, and 7S DNA (lower panel), as ratio of mtDNA+7S DNA over mtDNA, as previously described[3]. Mitochondrial DNA assets in *TWNK*-adPEO-P were not significantly altered compared to *TWNK*-adPEO and control subjects (one-way ANOVA and Tukey's multiple comparisons test, $P = 0.7826$, $P = 0.2621$, $P = 0.4012$, respectively).
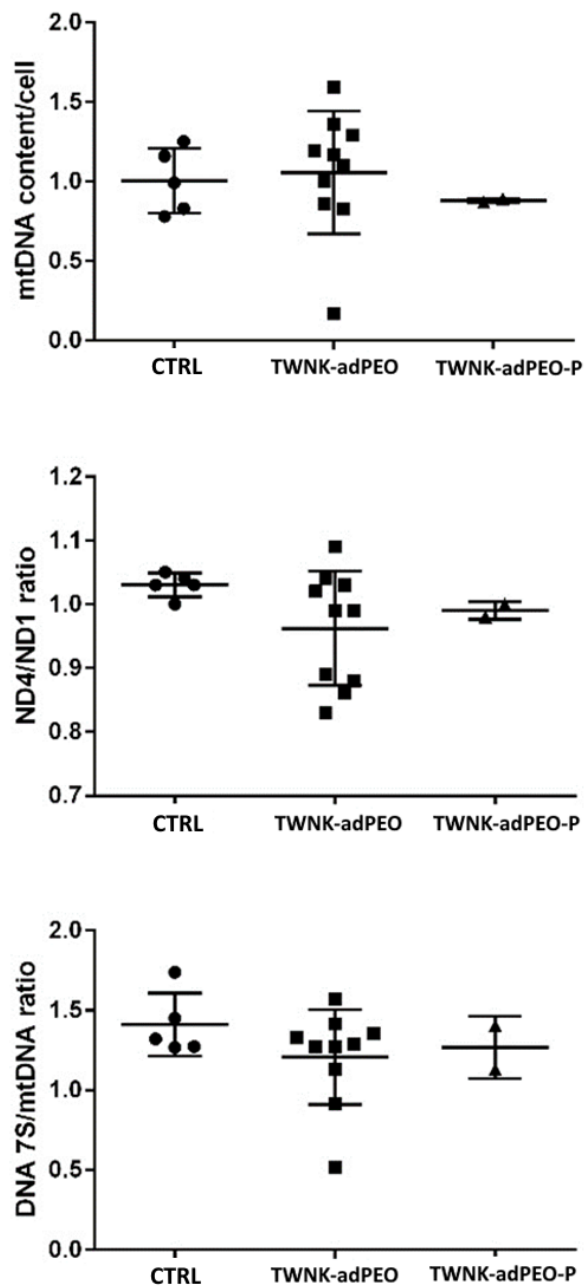
6. Supplementary Figure 3 (Fig. S3)

Structural analysis of variants in TWINKLE involved in PD.

(**A**) Structure of a hexameric TWINKLE aligned with the hexameric gp4 (PDB ID:1Q57). Five monomers of TWINKLE are shown in purple and pink in gp4 and one monomer in TWINKLE is blue and yellow in gp4. Please note that the N-terminal primase-like domain is not shown in the hexamer and the C-terminal end (residues 629-684) is unstructured according to the prediction (**B**) Structure of a TWINKLE monomer is shown in blue and gp4 is shown in yellow. The location of PD variants is indicated in pink and adPEO-P variants as gray spheres. (**C**) Left panel; L167 variant is shown in pink and nearby interacting amino acids are shown in red. Right panel; L169 has been mutated to proline leading to loss of interactions and making the protein more rigid. (**D**) Left panel; R371 (pink) variant possibly forms a salt bridge (thin line ≈ 4 Å) with amino acid E479 (red). R371 is located in an α-helix known to be essential for oligomerization. Neighboring residues (green) are known to cause disease when mutated. Right panel; R371 is changed to Q371 which leads to a molecular clash with E479 and provokes a destabilization of the hexamer. (**E**) Left panel; E461 (pink) forms a salt bridge with R394 (red). The thin line represents the salt bridge with a lenght of ≈ 1.9 Å. Right panel; E461 is changed to K461 leading to an electrostatic clash with R394. Neighboring residues (green) are known to cause disease when mutated. (**F**) Left panel; G540 variant is shown in pink. Please note that Gly has no side chain. Right panel; G540 is changed to R540 that has an extended side chain. This side chain will electrostatically clash with K578 (red) in an α-helix coming from the neighboring TWINKLE monomer (purple). Neighboring residue (green) is known to cause disease when mutated. (**G**) Multiple sequence alignment of the C-terminal (residues 629-684) of TWINKLE homologs in human, mouse, pig, bovine and chimpanzee. The location of K656Q and Q670H are highlighted in pink and

confirmed disease-causing mutations in the human variant in green. The conserved residues are marked with stars.
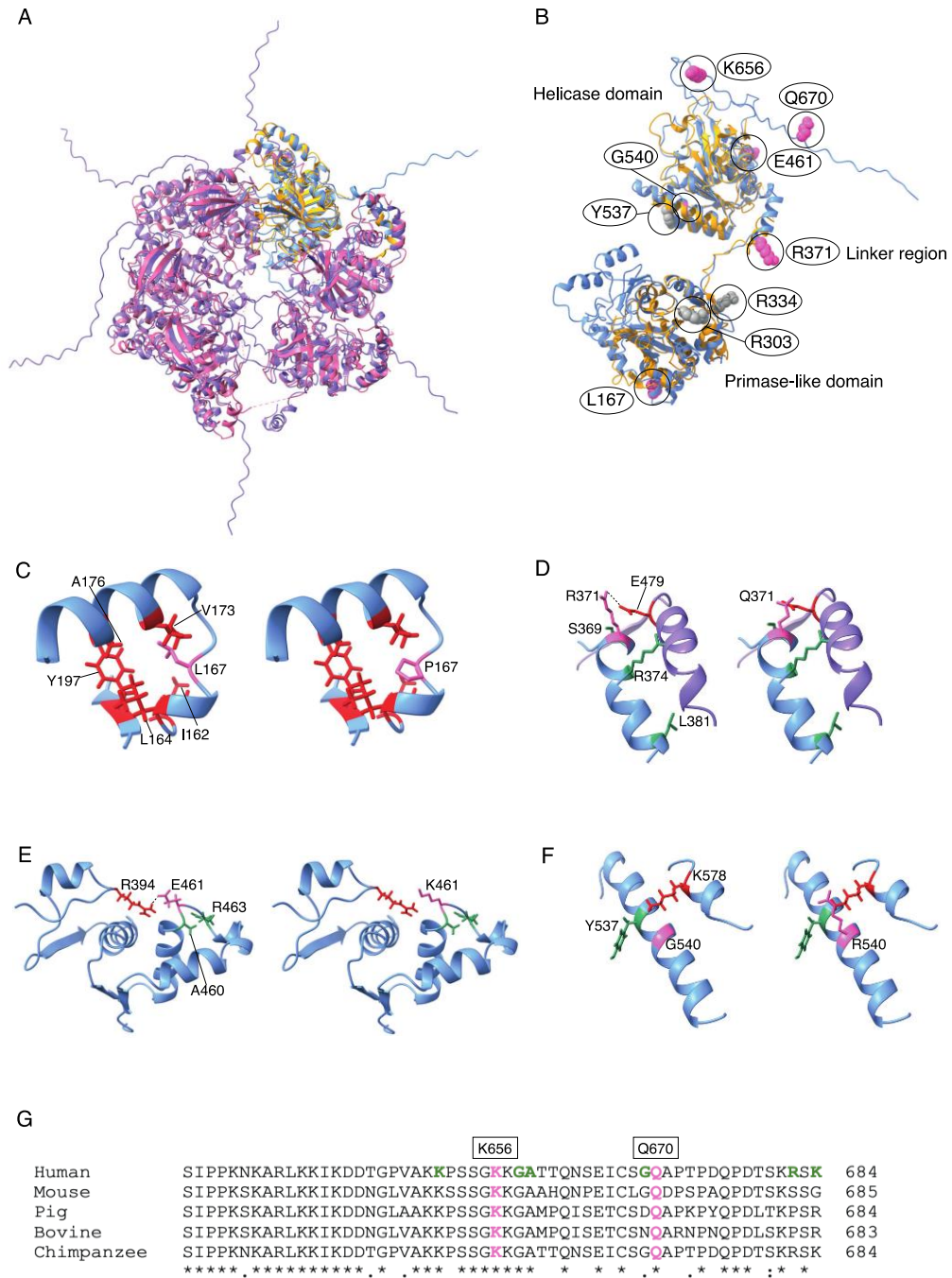
Supplementary References

1. Richards S, Aziz N, Bale S, et al. Standards and guidelines for the interpretation of sequence variants: A joint consensus recommendation of the American College of Medical Genetics and Genomics and the Association for Molecular Pathology. *Genet Med*. 2015;17(5):405-424. doi:10.1038/gim.2015.30

2. Ellard S, Baple EL, Callaway A, et al. ACGS Best Practice Guidelines for Variant Classification in Rare Disease 2020. In: *ACGS*. ; 2020.

3. Del Dotto V, Ullah F, Di Meo I, et al. SSBP1 mutations cause mtDNA depletion underlying a complex optic atrophy disorder. *J Clin Invest*. 2020;130(1):108-125. doi:10.1172/JCI128514

4. Giordano C, Iommarini L, Giordano L, et al. Efficient mitochondrial biogenesis drives incomplete penetrance in Leber's hereditary optic neuropathy. *Brain*. 2014;137(2):335-353. doi:10.1093/brain/awt343

5. Jumper J, Evans R, Pritzel A, et al. Highly accurate protein structure prediction with AlphaFold. *Nature*. 2021;596(7873):583-589. doi:10.1038/s41586-021-03819-2

6. Varadi M, Anyango S, Deshpande M, et al. AlphaFold Protein Structure Database: Massively expanding the structural coverage of protein-sequence space with high-accuracy models. *Nucleic Acids Res*. 2022;50(D1):D439-D444. doi:10.1093/nar/gkab1061

7. Korhonen JA, Pande V, Holmlund T, et al. Structure – Function Defects of the TWINKLE Linker Region in Progressive External Ophthalmoplegia. *J Mol Biol*. 2008;377:691-705. doi:10.1016/j.jmb.2008.01.035

8. Ingolia NT, Lareau LF, Weissman JS. Ribosome Profiling of Mouse Embryonic Stem

Cells Reveals the Complexity of Mammalian Proteomes. *Cell*. 2011;147(4):789-802. doi:10.1016/j.cell.2011.10.002.Ribosome

9.   Peter B, Falkenberg M. TWINKLE and other human mitochondrial DNA helicases: Structure, function and disease. *Genes (Basel)*. 2020;11(4). doi:10.3390/genes11040408

10.   Notarnicola SM, Mulcahy HL, Lee J, Richardson CC. The acidic carboxyl terminus of the bacteriophage T7 gene 4 helicase/primase interacts with T7 DNA polymerase. *J Biol Chem*. 1997;272(29):18425-18433. doi:10.1074/jbc.272.29.18425

11.   Loparo JJ, Kulczyk AW, Richardson CC, Van Oijen AM. Simultaneous single-molecule measurements of phage T7 replisome composition and function reveal the mechanism of polymerase exchange. *Proc Natl Acad Sci U S A*. 2011;108(9):3584-3589. doi:10.1073/pnas.1018824108

12.   Van Goethem G, Löfgren A, Dermaut B, Ceuterick C, Martin JJ, Van Broeckhoven C. Digenic progressive external ophthalmoplegia in a sporadic patient: Recessive mutations in POLG and C10orf2/twinkle [2]. *Hum Mutat*. 2003;22(2):175-176. doi:10.1002/humu.10246

13.   Baloh RH, Salavaggione E, Milbrandt J, Pestronk A. Familial Parkinsonism and Ophthalmoplegia From a Mutation in the Mitochondrial DNA Helicase Twinkle. *Arch Neurol*. 2007;64(7):998-1000.

14.   Liu Z, Ding Y, Du A, Zhang B, Zhao G, Ding M. A novel Twinkle (PEO1) gene mutation in a Chinese family with adPEO. *Mol Vis*. 2008;14:1995-2001.

15.   Vandenberghe W, Van Laere K, Debruyne F, Van Broeckhoven C, Van Goethem G. Neurodegenerative Parkinsonism and Progressive External Ophthalmoplegia with a

Twinkle Mutation. *Mov Disord*. 2009;24(2):308-309. doi:10.1002/mds.22275

16.   Brandon BR, Diederich NJ, Soni M, et al. Autosomal dominant mutations in POLG and C10orf2 : association with late onset chronic progressive external ophthalmoplegia and Parkinsonism in two patients. *J Neurol*. 2013;260:1931-1933. doi:10.1007/s00415-013-6975-2

17.   Kiferle L, Orsucci D, Mancuso M, et al. Twinkle mutation in an Italian family with external progressive ophthalmoplegia and parkinsonism : A case report and an update on the state of art. *Neurosci Lett*. 2013;556:1-4. doi:10.1016/j.neulet.2013.09.034

18.   Breen DP, Munoz DG, Lang AE. Twinkle-associated familial parkinsonism with Lewy pathology Cause or predisposition ? *Neurology*. 2020;95:644-647. doi:10.1212/WNL.0000000000010674

19.   Spinazzola A, Viscomi C, Fernandez-vizarra E, et al. MPV17 encodes an inner mitochondrial membrane protein and is mutated in infantile hepatic mitochondrial DNA depletion. 2006;38(5). doi:10.1038/ng1765